University of Exeter coursework header sheet

ECM3149 Commercial and Industrial Experience and Individual Project(BEng/MEng) (A, TRM1+2 2015/6)

011644

1019479

630004095

Coursework: Final report

Submission Deadline: Thu 28th Apr 2016 12:00

Personal tutor: Dr Maria Rosaria Marsico

Marker name: G Tab

Word count: 10558

By submitting coursework you declare that you understand and consent to the University policies regarding plagiarism and mitigation (these can be seen online at www.exeter.ac.uk/plagiarism, and www.exeter.ac.uk/mitigation respectively), and that you have read your school's rules for submission of written coursework, for example rules on maximum and minimum number of words. Indicative/first marks are provisional only.

Final Report

On the Production of Countermeasure Fins through the use of Additive Manufacture

Peter Michaelis Lewis

2016

3rd Year Individual Project

I certify that all material in this thesis that is not my own work has been identified and that no material has been included for which a degree has previously been conferred on me.

Signed.....

College of Engineering, Mathematics, and Physical Sciences
University of Exeter

Final Report

ECM3149

Title: On the Production of Countermeasure Fins through the use of Additive Manufacture
Word count: 10558
Number of pages: 30

Date of submission: Thursday, 28 April 2016

Student Name: Peter Michaelis Lewis
Programme: MEng Materials Engineering with Industrial Experience
Student number: 630004095
Candidate number: 011644

Supervisor: Dr Gavin Tabor

Acknowledgements

Without the support I received from Chemring Countermeasures, this project would have not been possible. As a result, I would firstly like to thank Andrew Barlow and Paul Minckley for their continued guidance, advice, and swift response to my queries. Along with Mick Robinson, for initiating this project as well as organising meetings between the relevant parties from Chemring Countermeasures and the University of Exeter.

Further to this, I would like to thank Dr Gavin Tabor, for the direction and motivation he provided through our weekly meetings. I would also like to thank: Tommy Shyng for his assistance with the tensile testing, Russell Edge for his support in the use of the CubePro®, and Paul McCutchion for the information he provided with regard to additive manufacture.

Finally, I am most grateful to Tim Gabbitas (Materialise), Tamlyn Verwey (CRDM), and Eric Edwards (3TRPD) for providing the requested quotations regarding the additive manufacture of fins.

Abstract

This project investigated the potential production of Chemring Countermeasures Ltd.'s fin components, through the use of additive manufacturing techniques. The aim was to assess the viability of additively manufacturing these parts, from both functional and economic viewpoints. Chemring Countermeasures' conceptual extended fin was taken as a fixed design, for the purpose of this study.

Following the identification of potentially suitable additively manufactured materials, a transient structural finite element analysis was undertaken. This was to assess whether a carbon filled nylon, produced through additive manufacture, would be able to withstand the loading on the fins during deployment. A mathematical model was developed and applied, in order to obtain values for the variation of loading with time from barrel exit.

The finite element analysis found the carbon filled nylon to be unsuitable, for the application of the fin component. However, it has been identified that this is due to stress concentrations at sharp edges. As a result, it has been recommended that Chemring Countermeasures re-design their fin, incorporating less sharp edges. This is likely to allow the implementation of additively manufactured polymer-based fin components, which have been shown to provide a cost-benefit over the current manufacturing method via an economic analysis. This analysis focused on Chemring Countermeasures outsourcing the manufacture of their fins, as they currently do.

In addition, a concept to eliminate the use of the retaining wire, for the fins, was proposed; and tensile testing undertaken to assess the ultimate tensile strength of this wire under launch conditions. This proved the concept to be a viable design option. Also, a study on the geometric suitably of the fin component to additive manufacture was undertaken. This used a CubePro® to prototype several fins, with moderate levels of success.

Keywords:

- Additive manufacture
- Rapid prototyping
- Mathematical modelling
- Finite element analysis
- Tensile testing
- Economic analysis

Table of Contents

1. Introduction and Background

A review of the in-service naval rounds produced by Chemring Countermeasures Ltd. (CCM) identified a scope for the use of additive manufacturing (AM); in the production of flight stabilising fins [1]. These fins are used in both CCM's rocket and mortared naval countermeasures. Four fins are located at the rear of the round; their function being to stabilise flight trajectory. Currently, CCM employ the fin design shown by figure 1.1. However, they are aiming to implement a new fin in the near future, which extends to wrap around the next fin. This design is given by figure 1.2. Prior to launch the fins are sealed with the use of a retaining wire. During launch this wire fails, releasing the fins. Upon exiting the barrel, the fins rotate outwards, by 118°, where they are locked in position. This deployment is mainly driven by the torque from a tangential leg spring (TLS).

Presently, the fins are manufactured by extrusion and subsequent subtractive machining. By implementing AM techniques, CCM would gain greater geometric freedom in their products; permitting "*design for function*" as oppose to "*design for manufacture*" [2]. Cost reduction may also be realised, along with shorter lead times. Moreover, components can be eliminated as individual parts and assemblies are combined, and manufactured in one go with the use of AM.

To provide structure to this project and report, Ashour Pour et al.'s evaluation framework for the implementation of AM was followed [3]. This model was chosen as it is aimed at companies "*approaching AM for the first time*", which applies to CCM. The basis of this is to first undertake a preliminary assessment, followed by technical and then economic studies.

A literature review is detailed in section 2 which highlights the relevant previous research, as well as drawing conclusions from this. Section 3 describes the methodology and theory behind the project, whilst identifying the need for each part of the project. Section 4 details how the project developed, from methods and theory into meaningful results. These results are presented throughout section 5, and are discussed in detail during section 6. In section 7, the conclusions that can be taken from this research are laid out, whilst providing recommendations for future studies. Section 8 presents the project management side to this study, it considers: project planning and sustainability, as well as the relevant health and safety aspects. Finally, the references used in delivering this report are listed.

Figure 1.1: CCM's current fin design.

Figure 1.2: CCM's new extended fin design.

2. Literature Review

2.1. Countermeasure Studies

CCM performed wind tunnel experiments to validate their flight stability calculations and trail their extended fin design [4]. Finding the concept fin to provide a more stable flight. Hence, this study has focused on the AM of the concept fin as opposed to the current design. These experiments also made it clear that using longer fins with lower mass will increase flight stability [4]. AM offers the possibility of reducing mass by using polymer-based materials, or by incorporating internal cavities, such as a honeycomb structure [2].

Johnson studied the trajectory of CCM's naval countermeasures, as well as the optimisation of fin design [5]. This provided data on the overall motion of a countermeasure during the deployment of the fins. In addition, it gave guidance on improving the aerodynamic performance of the fins. However, this study did not consider the practicality of the fin design. As the optimal design had high curvature, it would be difficult to implement into the current deployment system. On the other hand, if sufficient space exists in the launcher to fit Johnson's design in an open position, then AM would allow for the production of this complex geometry.

2.2. Methods for Additive Manufacture

The following groups of AM technologies exist: vat photo-polymerisation, powder bed fusion (PBF), extrusion-based, material jetting, binder jetting, sheet lamination, directed energy deposition, and direct write [2]. When processing metals, PBF systems are often employed [6]. Laser sintering (LS) and laser melting (LM) are the fundamental PBF technologies, whereby a laser is used to selectively sinter or melt powder layer-by-layer [2, 7-9]. Electron beam melting (EBM) [2, 9], and laser engineered net shaping (LENS) [2, 10] are also common. A limitation of PBF is the creation of thermal stresses in the part [11]. Recently, using extrusion-based systems, namely fused deposition modelling (FDM), particle-reinforced [2, 12] and even fibre-reinforced polymer composites have been successfully fabricated [13].

AM permits the entire volume of the part to be accessed throughout fabrication, and Meisel et al. investigated the insertion of functional components during the build process; developing a series of "*design for embedding*" considerations [14]. The TLS's presently used in the fin assembly are likely to be unsuitable for AM production; and hence a process of embedding these during fabrication, by pausing the build, may be a viable option.

2.3. Economics of Additive Manufacture

A generalised cost model for AM was outlined by Gibson et al. [2]. The costs realised were separated into four categories. These included; machine purchase, machine operation, material and labour. Cost models specific to producing polymer parts through stereo-lithography (SLA) [15], FDM [16], and LS [16-18] processes have been established. Whilst for metal parts, cost models have been developed for LS [19-23], LM [24], and EBM [23, 25] processes. These cost models provide the basis for an economic analysis into the viability of in-house AM.

Cost-benefit case studies comparing AM processes to conventional methods, in the form of breakeven analysis's; have verified that for low production volumes AM can be economically feasible [15-19, 26]. Initially, Hopkinson and Dickens found AM to be more suitable for low production volumes, assuming the cost per AM part to be independent of the number of parts [15, 16]. Ruffo et al. developed upon this; showing that the cost per AM part decreases with an increasing number of parts, based upon the LS process [17]. Step changes in cost per part were observed from their model, when increasing the number of parts required the use of another layer or machine. Atzeni and Salmi's group have also undertaken breakeven analysis case studies, but re-designed the parts to utilise AM's advantages [18, 19]. This showed that AM can be economically feasible for higher production volumes, using polymers [18] or metals [19]. However, these studies were based upon the Italian economy; so may not be entirely applicable to CCM. The most recent breakeven analysis by Lindemann et al., considered life-cycle costs; showing the step changes from Ruffo et al.'s model to be negligible [26]. Due to the rapid development of AM in recent years [27], these processes may have become more economically feasible since these cost-benefit studies, dated from 2001-2012, were undertaken.

A sensitivity analysis was undertaken by Schröder et al., finding the investment cost of the machine to be significant [28]. CCM could avoid this by outsourcing the AM, however in the long term it may be more cost-effective to make the investment into this rapidly developing technology. Moreover, Schröder et al.'s analysis showed that for small parts, post-processing in large volumes can be costly and that the number of parts has a relevance. Whilst for large parts the production quantity is nearly independent of cost per part [28].

The extensive study into the costs of AM, by Baumers et al., particularly focused on processing metals through EBM and LS [20-23]. They highlighted that available materials and processing rates, are the major bottlenecks to the AM of metal parts; this is in a purely economic [23]. Which agrees with Thomas and Gilbert's comprehensive literature review [29].

2.4. Implementation of Additive Manufacture

The underlying reason that AM technologies are not currently widely implemented, is that they lack competence to conventional methods; in terms of standardisation, surface roughness, processing rate, and raw materials [3]. It has also been noted that suppliers of polymer AM do not aim for as much consistency in their output as those producing metal parts [30].

A framework for implementation was put forward by Mellor et al.; this was based around five factors: AM strategy, AM technology, organisational change, systems of operations, and the AM supply chain [31]. In reference to this framework; a major challenge for a company such as CCM is in the understanding of AM's design constraints, whilst changing from a traditional production culture [31]. Achillas et al., also proposed an implementation framework [32]. Applying this to a specific SME, they identified that AM can provide a reliable solution for a low production volume; in agreement with the aforementioned cost-benefit studies [15-19, 26]. Furthermore, their results showed that AM reduces labour costs and could shift an SME from a "*make-on-stock*" to a "*make-on-demand*" strategy [32].

2.5. Hybrid and Integrated Manufacture

A hybrid manufacturing system is defined as "*the combination of manufacturing processes from different processing categories*" [33]. Often this takes the form of "*additive methods integrated with subtractive methods*" (AIMS) [25]. An AIMS system, namely LAMP, was presented by Nagel and Liou [33]. The authors stated several advantages of this system, over the individual processes, including: fabricating overhanging sections, reducing support structures, and embedding external features [33]. Manogharan et al., developed an economic model for an AIMS system; finding it to be suitable for processing expensive, hard to machine materials [25]. However, for AIMS systems to become more wide-spread, lower AM cost and quicker production times were identified as requirements by the authors [25].

A contrasting hybrid manufacturing method is to begin production of a product using AM; switching to a conventional method once the market demand has increased. This eliminates the risk of investing in expensive tooling, when the production volume is unpredictable. Khajavi et al. used the net present value of a product to analyse this type of production strategy [34]. They showed this hybrid method to cost around two-thirds of conventional manufacturing if re-design was required, and less than a fifth if the product was to be a failure. Additionally they outlined a methodology for deciding when to switch from AM to conventional production [34].

3. Methodology and Theory

3.1. Materials Selection

In order to get an idea of the material properties that can be realised through AM, research was undertaken into several UK based companies. CCM had previously trailed fins made from a polymer composite, namely 30% glass filled nylon (G-PA). These G-PA fins did withstand the temperatures of launch and flight, but failed mechanically on deployment. CCM currently use aluminium 6063T for the fins and this is proven to be reliable. However, reducing the mass of the fins would result in a more stable flight for the countermeasure [4]. As a result, this research aimed to identify materials for AM; with greater stiffness and strength than G-PA, whilst having lower density than aluminium. This identified four polymer-based materials that had a potential to be used for the fins. These materials are detailed in table 3.1. In addition the mechanical properties of AM aluminium are shown to vary between manufactures in table 3.1. This is due to Materialise recording data after a heat treatment, whereas 3TRPD's data is prior to any additional processing.

Table 3.1: Mechanical properties of candidate materials for AM fins. Data from CRDM [35], Materialise [36-38], 3TRPD [39].

Material	Aluminium Filled PA	Accura® 55	Somos® PerFORM	Carbon Filled PA	Aluminium ($AlSi_{10}Mg$) Before HT	Aluminium ($AlSi_{10}Mg$) After HT
Company	Materialise	CRDM	Materialise	Materialise	3TRPD	Materialise
Process	LS	SLA	SLA	LS	LS	3DP
Density / $g \cdot cm^{-3}$	1.4	1.2	1.6	1.1	2.7	2.7
Tensile Modulus / GPa	4	3	11	9	65	60
Tensile Strength / MPa	48	66	70	84	265	345
Yield Strength / MPa	-	-	-	-	170	230
Fracture Strain / %	3.5	6.5	1.1	3.8	4.0	11.0

To discover if any of the polymer-based materials in table 3.1 have the required mechanical properties to withstand deployment, more refined values for stresses and strains of the fin were required. Unfortunately, CCM could not provide data for the timescales of deployment, or the loading on the fins, expect for that from the TLS. As a result, a mathematical model was created and solved, and stresses found using computational methods.

3.2. Mathematical Model of Fin Deployment

A mathematical model was required to obtain values for the loading on the fins with time during deployment. This was so that the correct loading could be inputted into the computational analysis, to find the stresses on the fins during deployment. Ultimately, to assess the viability of utilising any of the polymer materials detailed in table 3.1.

Basic Model

The simplest method of modelling the fin deployment, is to only consider the torque from the TLS; the 'spring-only' condition. By Newton's 2nd law, this model is given by equation 3.1. Here, I is the fin's mass moment of inertia about the hinge points, θ is the rotation of the fin from the closed position, and t is the time from the bottom of the fins exiting the barrel. Whilst, k and ϕ represent the spring rate and angle of twist of the TLS, respectively. It should also be noted that 1 and 2 in subscript denote the value at the closed (θ_1) and deployed (θ_2) positions, respectively. By integrating equation 3.1 with respect to time, its solution found; which is given by equation 3.2. This is the theoretical time for deployment, considering only the TLS torque. By using the initial conditions of zero rotation ($\theta = 0$) and angular velocity ($\frac{\partial\theta}{\partial t} = 0$), at the closed position ($t = 0$), a theoretical deployment can be found by equation 3.3.

$$I \cdot \frac{\partial^2\theta}{\partial t^2} = k \cdot \left(\phi_1 - (\phi_1 - \phi_2) \cdot \frac{t}{t_2}\right) \quad \textbf{Eq. 3.1}$$

$$\theta = \frac{k}{6I} \cdot t^2 \cdot \left(3\phi_1 - (\phi_1 - \phi_2) \cdot \frac{t}{t_2}\right) \quad \textbf{Eq. 3.2}$$

$$t_2 = \sqrt{\frac{6 \cdot I \cdot \theta_2}{k \cdot (2 \cdot \phi_1 + \phi_2)}} \quad \textbf{Eq. 3.3}$$

Resistive Forces

By comparing the theoretical deployment time to an experimental time, the significance of resistive forces can be considered. The experimental time refers to the deployment time under ambient conditions. This, therefore, does not take into account any possible contributions to the deployment from the barrel pressure, or strong winds. However, it does permit an estimation of the collective magnitude of resistive forces, which include; friction between the fin and hinge pin, friction between the fin and fin cup, and drag opposing fin deployment. It should be noted that the drag experienced indoors, will differ to the actual deployment conditions.

If the experimental time is found to differ significantly from the theoretical time, it proves the resistive forces to be significant. In this case, the resistive forces would have to be accounted for in the mathematical model, as equation 3.4 depicts. A coefficient of resistance, denoted by C, is used. This assumes that the coefficient of resistance is constant, and solely dependent on the angular velocity of the fin. The solution to equation 3.4 is given by equations 3.5 and 3.6. When the time is set equal to the experimental deployment time ($t = t_2$), an iterative approach can be employed to obtain the value of the coefficient of resistance.

$$I \cdot \frac{\partial^2 \theta}{\partial t^2} + C \cdot \frac{\partial \theta}{\partial t} = k \cdot \left(\phi_1 - (\phi_1 - \phi_2) \cdot \frac{t}{t_2}\right) \quad \textbf{Eq. 3.4}$$

$$\theta = \frac{k}{C} \cdot \left(\phi_c \cdot g(t) - \frac{\phi_1 - \phi_2}{t_2} \cdot \left(\frac{t^2}{2} - \frac{I}{C} \cdot g(t)\right)\right) \quad \textbf{Eq. 3.5}$$

$$g(t) = t + \frac{I}{C} \cdot \left(e^{-\frac{C}{I} \cdot t} - 1\right) \quad \textbf{Eq. 3.6}$$

On the other hand, if the difference between experimental and theoretical deployment times is deemed to be suitably small, the resistive forces are proved to be negligible. In this case equation 3.2 provides a suitable mathematical model for fin deployment; it considers only the TLS torque, and resistive forces opposing fin rotation.

Pressure

The only potentially significant loading on the fins during deployment, yet to be considered is the barrel pressure. The importance of this can be assessed by comparing the experimental and actual deployment times. The actual time will consider all relevant loading on the fins, including; the aforementioned resistive forces, but also the contribution of the barrel pressure.

This method of assessing the loading on the fins by comparing: theoretical, experimental, and actual deployment times; is capable of leading to one of four potential mathematical models. Firstly, the scenario of both the resistive forces and barrel pressure being considered significant. In this case the mathematical model is depicted by equation 3.7. This assumes the pressure is acting solely over the entire inner face, and decreases linearly with time to zero once the fins are fully deployed. The solution to equation 3.7 is given by equation 3.8. In these equations, p_1 denotes the pressure experienced when the fins are in the closed position ($t = 0$), A_i is the area of the fin's inner face, and l_z is the perpendicular distance from the centroid of l_z to the axis of rotation. Further to this, $g(t)$ is given by equation 3.6.

$$I \cdot \frac{\partial^2 \theta}{\partial t^2} + C \cdot \frac{\partial \theta}{\partial t} = k \cdot \left(\phi_1 - (\phi_1 - \phi_2) \cdot \frac{t}{t_2}\right) + p_1 \cdot A_i \cdot l_z \cdot \left(1 - \frac{t}{t_2}\right) \quad \textbf{Eq. 3.7}$$

$$\theta = \frac{k}{C} \cdot \left(\phi_1 \cdot g(t) - \frac{\phi_1 - \phi_2}{t_2} \cdot \left(\frac{t^2}{2} - \frac{I}{C} \cdot g(t)\right)\right) - \frac{p_1 \cdot A_i \cdot l_z}{C \cdot t_2} \cdot \left(\frac{t^2}{2} - g(t)\right) \quad \textbf{Eq. 3.8}$$

The second scenario is a significant pressure, combined with negligible resistive forces; this gives the mathematical model portrayed by equation 3.9. The solution to this is given by equation 3.10. It is also possible for the contribution of the barrel pressure to be negligible, but the resistive forces to be significant. In this case equation 3.5 stands. Finally, if neither the barrel pressure nor resistive forces, were found to significantly affect the deployment of the fins, the theoretical 'spring-only' solution, given by equation 3.2, would be suffice.

$$I \cdot \frac{\partial^2 \theta}{\partial t^2} = k \cdot \left(\phi_1 - (\phi_1 - \phi_2) \cdot \frac{t}{t_2}\right) + p_1 \cdot A_i \cdot l_z \cdot \left(1 - \frac{t}{t_2}\right) \quad \textbf{Eq. 3.9}$$

$$\theta = \frac{k}{C} \cdot \phi_1 \cdot g(t) - \frac{p_1 \cdot A_i \cdot l_z}{C \cdot t_2} \cdot \left(\frac{t^2}{2} - g(t)\right) \quad \textbf{Eq. 3.10}$$

Calculation of the Pressure Constant

If the appropriate mathematical model for fin deployment contains the p_1 term, its value can now be obtained. This is done by using the conditions of the deployed position. These being; time equal to the actual deployment time ($t = t_2$), and rotation equal to that at the deployed position ($\theta = \theta_2$). In the scenario of both pressure and resistive forces being significant; equation 3.8 describes the fin rotation, with p_1 being obtained by equation 3.11. If the pressure is significant, but the resistive forces are not; equation 3.10 describes the fin rotation and equation 3.12 can be used to find p_1. Moreover, $g(t_d)$ is given by equation 3.13.

$$p_1 = \frac{t_2 \cdot \left(k \cdot \left(\phi_1 \cdot g(t_2) - \frac{\phi_1 - \phi_2}{t_2} \cdot \left(\frac{t_2^2}{2} - \frac{I}{C} \cdot g(t_2)\right)\right) - C \cdot \theta_2\right)}{A_i \cdot l_z \cdot \left(\frac{t_2^2}{2} - g(t_2)\right)} \quad \textbf{Eq. 3.11}$$

$$p_1 = \frac{t_2 \cdot (k \cdot \phi_1 \cdot g(t_2) - C \cdot \theta_2)}{A_i \cdot l_z \cdot \left(\frac{t_2^2}{2} - g(t_2)\right)} \quad \textbf{Eq. 3.12}$$

$$g(t_2) = t_2 + \frac{I}{C} \cdot \left(e^{-\frac{C}{I} \cdot t_2} - 1\right) \quad \textbf{Eq. 3.13}$$

3.3. Finite Element Analysis

The stresses present in load-bearing components are often studied using computational methods, in particular finite element (FE) analysis. Therefore, to assess the potential use of one of the polymer-based materials, given in table 3.1, an FE analysis may be used. This would also provide an increased knowledge of the currently grey area of fin deployment. The mathematical model, presented in section 3.2, provides a basis for obtaining the variation of loading with time. Further to this, Johnson's trajectory study permits the overall motion of the countermeasure to be included [5].

3.4. Elimination of Retaining Wire

One way in which AM can be utilised to reduce production costs and lead times is the combination of multiple parts into one [2]. This can be applied here by combining the four fins, and retaining wire into one part, by having a thin overlapping section joining each fin to the next. The creation of an accurate design, based upon this concept, requires a knowledge of the fracture stress of the retaining wire under launch conditions. However, as with fin deployment, there is a lack of detailed knowledge as to what happens to the retaining wire.

The current theory is that the initial launch pressure is responsible for the fins being forced outward to the inner barrel wall, and the retaining wire is broken at this point. Normally, it is found in the bottom of the barrel post firing as debris, however sometimes it is ejected. If ejected, the trajectory of retaining wire is random; hence creating a risk to the ship's crew. Although the wire is small, a high velocity post-launch will give it significant momentum. Moreover, sharp edges may exist following fracture, which could be considered as shrapnel. A thin overlapping section that fractures in a consistent, controlled manner during launch would eliminate this risk; whilst providing additional benefits in terms of cost reduction.

The fracture stress of the retaining wire under the conditions of launch can be approximated, through the use of a steady tensile test, at varying strain rates. With the aim of extrapolating the obtained data, to the strain rate of the retaining wire at launch; which is approximated by equation 3.14. Where, $\dot{\varepsilon}$ is the strain rate of the retaining wire, D_0 is the diameter of the 4 fins when sealed by the retaining wire, D_1 is the inner diameter of the launch barrel, and t_f is the estimated time at which the retaining wire fractures after launching.

$$\dot{\varepsilon} = \frac{\pi(D_1 - D_0)}{t_f} \qquad \textbf{Eq. 3.14}$$

3.5. Suitability for Additive Manufacture

When investigating the viability of AM for any part, is crucial to assess the suitability of that part for AM. The previously outlined sections of this project focus mainly on the materials selection for AM fins; assuming that the geometry is suitable, and that AM makes economic sense to CCM. Hence, these two key areas of implementing AM have also been analysed.

Geometric Suitability

Although AM technologies can provide many advantages to SMEs, such as CCM, they do not come without their limitations. One being that not all geometry can be fabricated successfully, despite AM generally providing a greater level of geometric freedom [2]. Resulting in some parts requiring re-design, in order to fully realise the benefits of AM, in a functional and economic sense [18, 19]. This provides a motivation to trail AM as a production method of CCM's fins, before committing to new manufacturing systems.

This has been done by using an extrusion-based system, namely CubePro® from 3D Systems Inc.; which is typically used for rapid prototyping in polymer materials. This provided a low-cost method of assessing the suitability of the fin component for AM, in terms of its geometry.

Economic Suitability

The most important factor affecting the suitability of AM, is arguably whether or not a cost benefit can be realised. As discussed in section 2.3, the literature consistently shows that for low-volume production, AM is often an economically viable production solution [15-19, 26]. The conclusions drawn from literature were based upon case studies, relating to a specific part or selection of parts; and hence the results are not generalised. Consequently, a cost-benefit case study directly related to CCM's fin component, is required in order to assess the economic viability of AM for its production.

Two methods of utilising AM exist for CCM. One being to purchase the relevant AM machine and materials; leading to the production of the fins in-house. The other being to outsource the AM to a company that specialise in this. The major advantage of the first option is that the production cost per part will be much lower. However, the initial purchase of the machine will be expensive. Moreover, as was identified in section 2.4, the literature highlights that a company such as CCM may find it difficult to undertake successful AM themselves [31]. As a result, the economic analysis presented in this report, focuses on contracting external companies to undertake the relevant AM.

4. Project Development

4.1. Application of Mathematical Model

Finding t_2, C, and p_1

The theoretical, experimental, and actual deployment times, defined in section 3.3, were found to be 17.8, 110.0, and 11.0 ms, respectively. The values used in the calculation of the theoretical time, by equation 3.3, can be seen in table 4.1; as can all of the values for calculations deliberated in this section. A comparison between the three deployment times highlights large enough differences, between all values, to warrant the use of the most advanced mathematical model; that given by equations 3.6-3.8.

Table 4.1: Values for the constants used in the mathematical model of fin deployment.

Constant	Value	Constant	Value	Constant	Value
I	$1.01 \times 10^{-4} / kg \cdot m^2$	ϕ_1	$5.03 / rad$	θ_2	$2.06 / rad$
k	$0.302 / N \cdot m \cdot rad^{-2}$	ϕ_2	$2.97 / rad$	A_i	$1.13 \times 10^{-2} / m^2$
ν	$1.51 \times 10^{-5} / m^2 \cdot s^{-1}$	ρ	$1.20 / kg \cdot m^{-3}$	A_o	$1.20 \times 10^{-2} / m^2$
l_z	$4.44 \times 10^{-2} / m$	R	$0.102 / m$	x	$8.64 \times 10^{-3} / m$

With the mathematical model decided upon, values for the coefficient of resistance C, and initial pressure p_1, could be obtained. In the calculation of p_1, it was assumed that l_z is the distance from the centre of gravity to the axis of rotation, as opposed to that of the centre of area. By applying an iterative approach to equation 3.5, with the time set to the experimental deployment time ($t = t_2$); the value of C was obtained, as the rotation θ tended towards the deployed position θ_2 ($\theta \to \theta_2$). A value for p_1 was subsequently obtained through the use of equations 3.11 and 3.13. The final values for t_2, C, and p_1, can be viewed in table 4.2.

Table 4.2: Final values for the parameters calculated from the mathematical model.

Parameter	Value	Parameter	Value	Parameter	Value
t_1	$1.10 \times 10^{-2} / s$	C	$6.38 \times 10^{-2} / kg \cdot m^2 \cdot s^{-1}$	p_1	$279 / Pa$

Variation of Loading with Time

The reason for developing this mathematical model was to obtain values for the varation of loading on the fins during deployment. Hence, once the parameters given in table 4.2 were finalised, the loading due to fin deployment was broken into three distinct categories: TLS torque, pressure, and resistive forces. The variation of TLS torque τ, and pressure p, with time; were found by equations 4.1 and 4.2, respectively.

$$\tau = k \cdot \left(\phi_1 - (\phi_1 - \phi_2) \cdot \frac{t}{t_2}\right) \quad \textbf{Eq. 4.1} \qquad p = p_1 \cdot \left(1 - \frac{t}{t_2}\right) \quad \textbf{Eq. 4.2}$$

The drag and frcition constitute the resitive forces, chacterised by C. They are in direct relation to the angular velocity $\frac{\partial\theta}{\partial t}$. Hence, equations 3.6 and 3.8 were differentiated to obtain equations 4.3 and 4.4, providing an expression for $\frac{\partial\theta}{\partial t}$. Subsequently, the variation of resitive force F with time, was found by eqaution 4.5. This method assumes the sumative effects of lateral drag $F_{D\vdash}$ and friction F_f, to be equivalent to a point load at the centre of gravity.

$$\frac{\partial\theta}{\partial t} = \frac{k}{C} \cdot \left(\phi_1 \cdot g'(t) - \frac{\phi_1 - \phi_2}{t_2} \cdot \left(t - \frac{I}{C} \cdot g'(t)\right)\right) - \frac{p_1 \cdot A_i \cdot l_z}{C \cdot t_2} \cdot (t - g'(t)) \quad \textbf{Eq. 4.3}$$

$$g'(t) = 1 - e^{-\frac{C}{I} \cdot t} \quad \textbf{Eq. 4.4} \qquad F = F_{D\vdash} + F_f = \frac{C}{l_z} \cdot \frac{\partial\theta}{\partial t} \quad \textbf{Eq. 4.5}$$

Breakdown of Resistive Loading

To assess the relative breakdown of resistive forces, the Reynolds number Re for the fin deployment was found, through equation 4.6. Here, R is the maximum radius of the fin, x is the maximum thickness of the fin, and ν is the kinematic viscosity of air. This gave a maximum Reynolds number ($Re_{max} \cong 10^4$) lower than 10^5, hence the flow was considered to be laminar. As a result, variation of lateral drag force with time could be approximated by equation 4.7 [40]. Where, ρ is the density of air, and A_o is the area of the fin's outer face. It should be noted that fluid properties were taken for a temperature of 20℃ [40], and their values are given in table 4.2. From this the variation of drag and friction with time were known.

$$Re = \frac{R \cdot \frac{\partial\theta}{\partial t} \cdot x}{\nu} \quad \textbf{Eq. 4.6}$$

$$F_{D\vdash} = 0.665 \cdot \rho \cdot A_o \cdot \sqrt[5]{\frac{\nu}{x} \cdot \left(R \cdot \frac{\partial\theta}{\partial t}\right)^9} \quad \textbf{Eq. 4.7}$$

4.2. Simulation Setup

A transient structural analysis was chosen over the less computationally expensive static option, to best consider the variance of the loading with time. The model was solved for maximum principal stress, using the Mechanical ANSYS Parametric Design Language (APDL). Material properties were based upon carbon filled nylon (C-PA) [38]; this was due to the high tensile strength, in comparison to other polymers in table 1.1. However, a Poisson's ratio of 0.25 was assumed, from data on carbon-fibre reinforced polymers [41].

The geometry used was as an assembly, made up of the extended fin located on the hinge pin. This was to create the most realistic representation of fin deployment. The movement of these two parts was defined using joints. Body-ground relationships were created for both parts, with the pin being fixed to the ground, whilst the fin was assigned revolute connections to the ground. In addition, a revolute body-body joint was created between the fin and the hinge pin.

From Johnson's study on countermeasure trajectory the velocity of the countermeasure was seen to be around $180\ m \cdot s^{-1}$ as it leaves the launcher [5]. Hence, this was inputted as an initial condition. Furthermore, an angular velocity, due to spin, of $0.02\ rad \cdot s^{-1}$ was inputted from these results [5]. From the gradient of Johnson's velocity-time plot the countermeasure acceleration was deduced as -10.3 $m \cdot s^{-2}$, in the direction of countermeasure motion [5]. This was combined with a lateral acceleration of $g \cdot \sin 45°$; which assumed a launch angle of $45°$.

The drag force acting on the top face of the fin was also considered. Based upon the velocity of $180\ m \cdot s^{-1}$ [5], the flow over the fin was shown to be turbulent ($Re \cong 10^6$), in the direction of countermeasure motion. This provided two empirical equations for the calculation of the skin friction coefficient [40]. The mean of these was taken to best estimate the drag force acting on the top face of the fin $F_{D\parallel}$, which is given by equation 4.8. Where, h is the height of the fin ($0.1045\ m$), and U denotes the countermeasure velocity. Giving a drag force of around $1.81\ N$.

$$F_{D\parallel} = (4.20875 \times 10^{-3}) \cdot \rho \cdot R \cdot h \cdot U^2 \cdot Re^{-0.2} \cdot (\log_{10} Re)^{-2.58} \qquad \textbf{Eq. 4.8}$$

The deployment time of $11\ ms$ was broken down incrementally into 20 time steps of $0.55\ ms$, for this analysis. The time from barrel exit and loading, from the mathematical model, at each step can be viewed in table 4.1. The countermeasure's acceleration and angular velocity, along with $F_{D\parallel}$ were inputted as constants. Although some of the loading had low values, all loading was included to ensure a complete model. Despite the potential to exclude the drag forces and angular velocity of the countermeasure to reduce computational expense.

Table 4.3: Breakdown of time steps and time-dependent loads, used in the FE analysis. It should be noted that the values presented are rounded, in the actual analysis a greater degree of accuracy was used.

Step Number	Step End Time / ms	TLS Torque / $N \cdot m$	Pressure / Pa	Friction / N	Lateral Drag / mN
0	0.00	1.52	279	0	0
1	0.55	1.49	265	94	83
2	1.10	1.46	251	161	216
3	1.65	1.42	238	207	342
4	2.20	1.39	224	240	445
5	2.75	1.36	210	262	524
6	3.30	1.33	196	278	582
7	3.85	1.30	182	289	623
8	4.40	1.27	168	296	652
9	4.95	1.24	154	301	672
10	5.50	1.21	140	305	685
11	6.05	1.18	126	307	694
12	6.60	1.14	112	308	699
13	7.15	1.11	98	309	701
14	7.70	1.08	84	309	702
15	8.25	1.05	70	309	701
16	8.80	1.02	56	308	700
17	9.35	0.99	42	308	698
18	9.90	0.96	28	307	695
19	10.45	0.93	14	306	693
20	11.00	0.90	0	306	690

The TLS torque was applied to the face of the groove on the fin's inner face. The pressure was applied over the entire inner face, whilst the lateral drag was applied over that of the outer face. The drag force parallel to countermeasure motion was applied on the top face. Finally, the accelerations and velocity were applied to the whole model, including the hinge pin.

4.3. Mesh Convergence Study

A mesh convergence study was undertaken to ensure that the results obtained from the transient structural FE analysis had mesh-independence, and were accurate. The maximum tensile and compressive stresses at each of the 20 time steps, were used to measure the convergence of the mesh. Initially a coarse mesh with of global element size of 10 mm was employed, and the number of elements was approximately doubled with each subsequent run. The final mesh had a global element size of 1.30 mm, with a 0.65 mm element size for faces previously displaying high stresses. Moreover, a first level of refinement was added to faces with sharp edges, with a second level for the face taking the TLS torque. The final mesh had 747,115 elements and 1,139,898 nodes. The mesh convergence is summarised by figure 4.1.

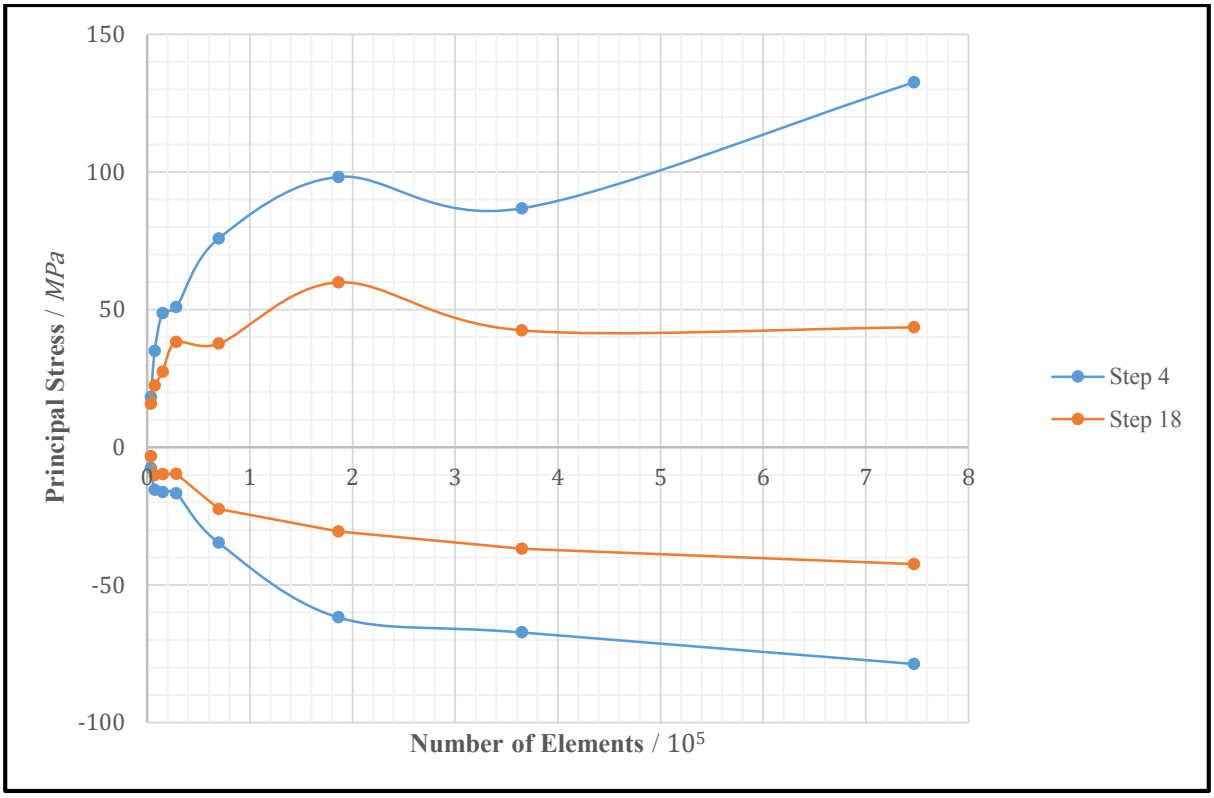

Figure 4.1: Mesh convergence results for step 4 (2.20 ms), and step 18 (9.90 ms); in terms of maximum tensile and compressive stress, and number of elements. These were chosen as they had the highest and lowest magnitudes of stress.

As figure 4.1 shows, the final mesh displayed a noticeable change in maximum tensile stress from the previous one. However, due to a bottleneck of the computing systems available, further refinement of the mesh would have become too computationally expensive. In addition, the average change in maximum tensile stress was only around 10 MPa for the final mesh. This was deemed to be an acceptable level of accuracy, considering the scope of this analysis.

4.4. Tensile Testing

An EZ20 universal testing machine was used for the tensile testing of the retaining wire. The retaining wire is stranded stainless steel A4-AISI 316 1.4401, with diameter of $0.81\ mm$. The samples were cut to $50\ mm$ lengths. Due to the small diameter it was necessary to test the grip-ability of the samples. Hence, 3 trail tests were performed at a strain rate of $50\ mm \cdot min^{-1}$. These 3 trail samples gave consistent results, and it was decided that grip was not an issue.

Due to the consistency in the trail tests, it was decided that they would be included in the results. A further 10 samples were tested, with 2 samples being tested at each of the following strain rates: 100, 250, 500, 750, and $1000\ mm \cdot mm^{-1}$.

The retaining wire's strain rate was estimated under the assumption that, the time for its fracture is the same as that for deployment ($t_f = t_d$). By inputting the relevant dimensions ($D_0 = 130.2\ mm$, $D_1 = 131.5\ mm$) into equation 3.14, the strain rate was approximated to be around $2 \times 10^4\ mm \cdot min^{-1}$. Based upon this the results were extrapolated and the ultimate tensile stress (UTS) of the retaining wire, under launch conditions, was approximated. Based upon this, the required cross-sectional area of the proposed overlap concept was found.

4.5. CubePro® Prototyping

Using a CubePro®, and its accompanying software, 8 extended fins were fabricated, along with a part made up of the fin cup and hinge pins. It should be noted than only part of the fin cup was fabricated, in order to reduce printing time.

The materials used were ABS and PLA. Furthermore, several parameters were varied; which included: resolution, print strength, print pattern, support type, support borders, and support angle. This was mainly a qualitative analysis, focusing on the suitability of the fin geometry. However, the quantitative parameters of: fabrication time, and part mass were also recorded.

4.6. Economic Analysis

Rough order of magnitude (ROM) cost quotations were obtained for fin production through a number of process. Apsely Precision Engineering Ltd. provided an ROM quotation for the traditional method of extrusion and machining. In terms of AM processes, contact was made with: Materialise, CRDM, and 3TRPD. This allowed all of the AM materials given in table 3.1, to be included in the analysis, and be compared to the traditional method.

5. Results

5.1. *Finite Element Analysis*

Table 5.1: Variation of the magnitude of maximum tensile and compressive stress, for a carbon-filled PA AM fin; including estimated error.

Time / ms	0	0.55	1.10	1.65	2.20	2.75	3.30
Tensile Stress / MPa	-	69 ± 4	81 ± 5	112 ± 27	132 ± 46	110 ± 30	98 ± 21
Compressive Stress / MPa	-	66 ± 9	72 ± 10	78 ± 11	79 ± 11	75 ± 11	72 ± 11
Time / ms	3.85	4.40	4.95	5.50	6.05	6.60	7.15
Tensile Stress / MPa	86 ± 17	68 ± 5	57 ± 3	57 ± 2	62 ± 2	86 ± 19	99 ± 29
Compressive Stress / MPa	67 ± 10	61 ± 9	55 ± 7	54 ± 7	57 ± 7	62 ± 8	63 ± 9
Time / ms	7.70	8.25	8.80	9.35	9.90	10.45	11.00
Tensile Stress / MPa	93 ± 28	72 ± 15	54 ± 5	49 ± 5	44 ± 1	44 ± 1	47 ± 0
Compressive Stress / MPa	60 ± 9	55 ± 9	50 ± 8	45 ± 7	42 ± 6	41 ± 4	43 ± 5

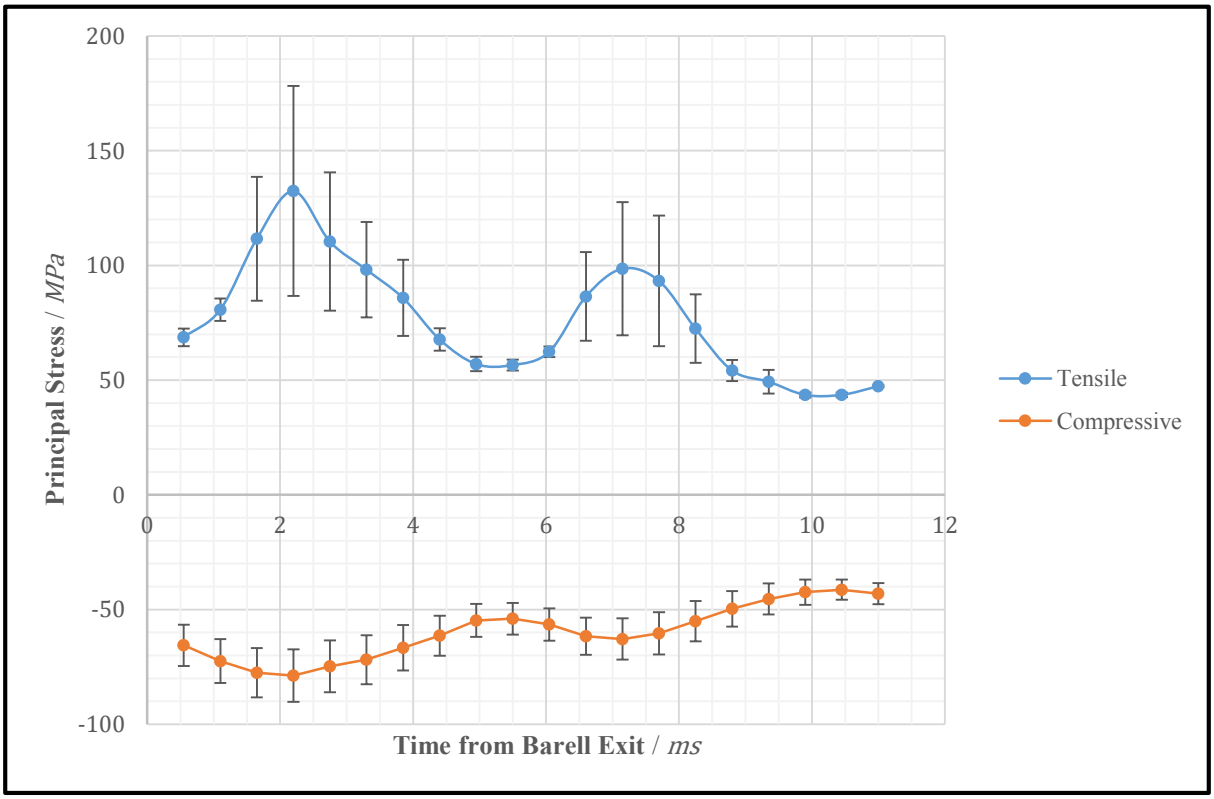

Figure 5.1: Maximum tensile stress in fin over deployment time, showing estimated error in stress.

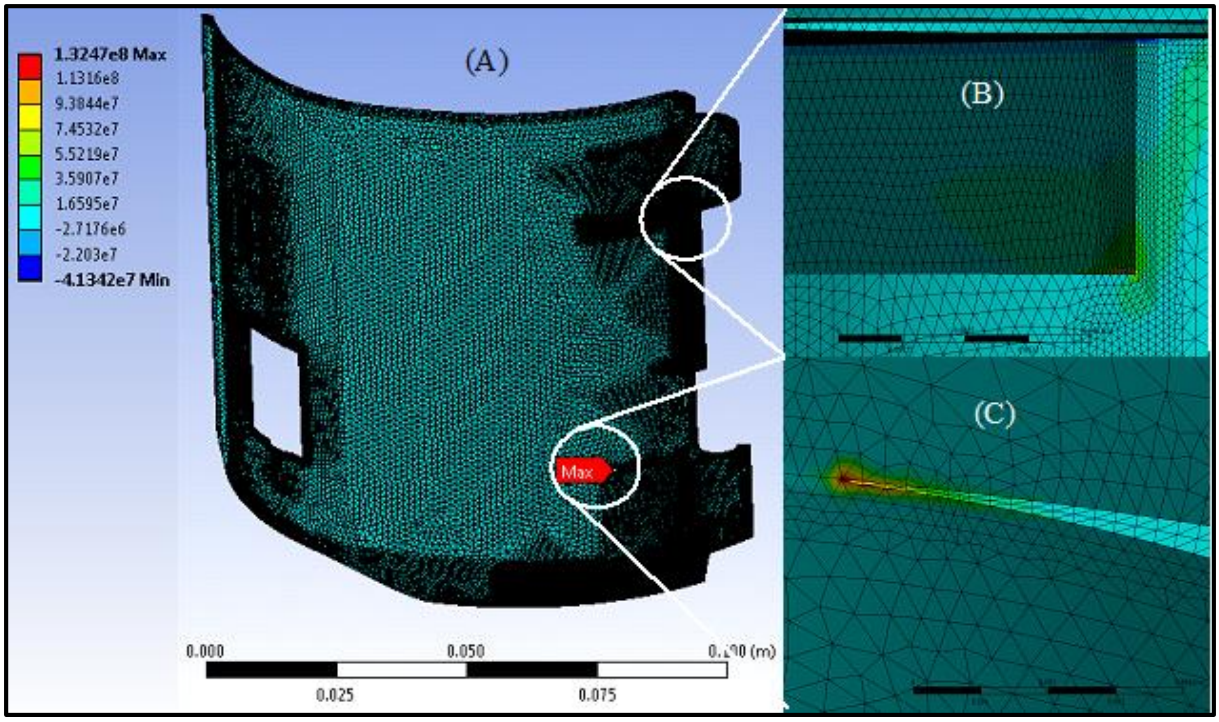

Figure 5.2: Maximum principal stress distribution at $t = 2.20\ ms$. (A) Inner face, showing the final mesh and location of maximum. (B) Zoomed in image of the edge of groove, under the upper hinge, where the TLS torque acts. (C) Zoomed in image of maximum stress, located on the top face of the lower hinge.

5.2. Tensile Testing

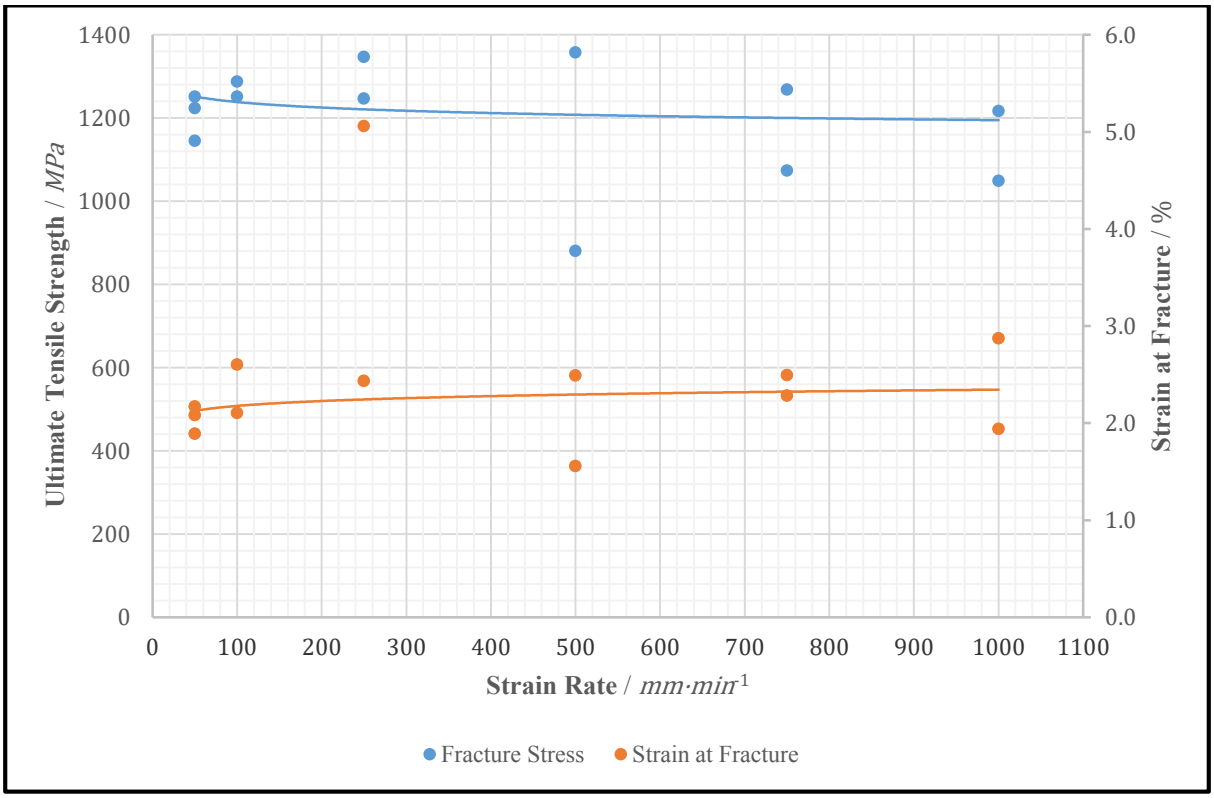

Figure 5.3: Ultimate tensile strength and strain at fracture of retaining wire, against strain rate. It should be noted that anomalous results have not been considered for the curves of best fit.

Table 5.2: Variation of ultimate tensile strength and strain at fracture, of the retaining wire, with strain rate; including error. It is should be noted that these results exclude anomalous results.

Strain Rate / $mm \cdot min^{-1}$	50	100	250	500	750	1000
Ultimate Tensile Strength / MPa	1206 $\pm$61	1269 $\pm$18	1297 $\pm$50	1357 $\pm$62	1172 $\pm$98	1132 $\pm$84
Strain at Fracture / %	2.07 $\pm$0.16	2.35 $\pm$0.25	2.40 $\pm$0.23	2.05 $\pm$0.45	2.40 $\pm$0.10	2.40 $\pm$0.50

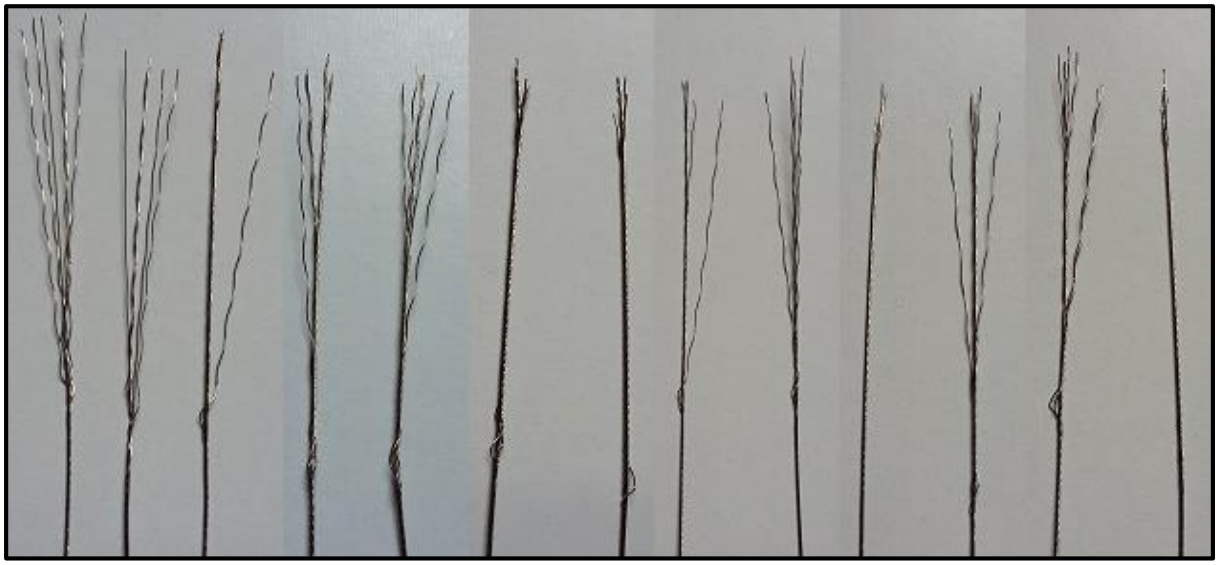

Figure 5.4: Photos of retaining wire samples, post tensile testing, with increasing strain rate from right to left. From right to left: Trail 1, Trail 2, Trail 3 ($50\ mm \cdot min^{-1}$); Sample 1, Sample 6 ($100\ mm \cdot min^{-1}$); Sample 2, Sample 7 ($250\ mm \cdot min^{-1}$); Sample 3, Sample 8 ($500\ mm \cdot min^{-1}$); Sample 4, Sample 9 ($750\ mm \cdot min^{-1}$); Sample 5, Sample 10 ($1000\ mm \cdot min^{-1}$).

Table 5.3: Ultimate tensile strength and breaking force for the retaining wire, under launch conditions.

Estimated Strain Rate / $mm \cdot min^{-1}$	Ultimate Tensile Strength / MPa	Breaking Force / N
2×10^4	1136	745

Table 5.4: Cross-sectional area, and thickness, of overlap for proposed concept.

Material	Aluminium Filled PA	Accura® 55	Somos® PerFORM	Carbon Filled PA	Aluminium ($AlSi_{10}Mg$) Before HT	After HT
Company	Materialise	CRDM	Materialise	Materialise	3TRPD	Materialise
Process	LS	SLA	SLA	LS	LS	3DP
Cross-sectional Area / mm^2	15.5	11.3	10.6	8.9	2.8	2.2
Thickness / μm	149	108	102	85	27	21

5.3. CubePro® Prototyping

Table 5.5: Prototyping parameters and results, displaying: print number, key build parameters, build time, and part mass. It should be noted that the fabrication of fin 6 failed.

No.	Alignment	Material	Resolution (μm)	Print Strength	Print Pattern	Support Type	Time ($h:m$)	Mass (g)
1	Vertical	PLA	200	Strong	Diamonds	Lines	02:52	32
2	Vertical	PLA	200	Strong	Honeycomb	Lines	04:57	45
3	Vertical	PLA	200	Strong	Honeycomb	Points	04:05	31
4	Horizontal	PLA	200	Strong	Honeycomb	Points	04:47	33
5	Vertical	ABS	200	Almost Solid	Honeycomb	Points	03:50	28
6	Angled	ABS	200	Strong	Diamonds	Points	-	-
7	Vertical	ABS	200	Strong	Honeycomb	Points	03:46	27
8	Vertical	PLA	70	Solid	Honeycomb	Points	07:38	32
Cup	-	PLA	300	Hollow	Honeycomb	Points	06:48	74

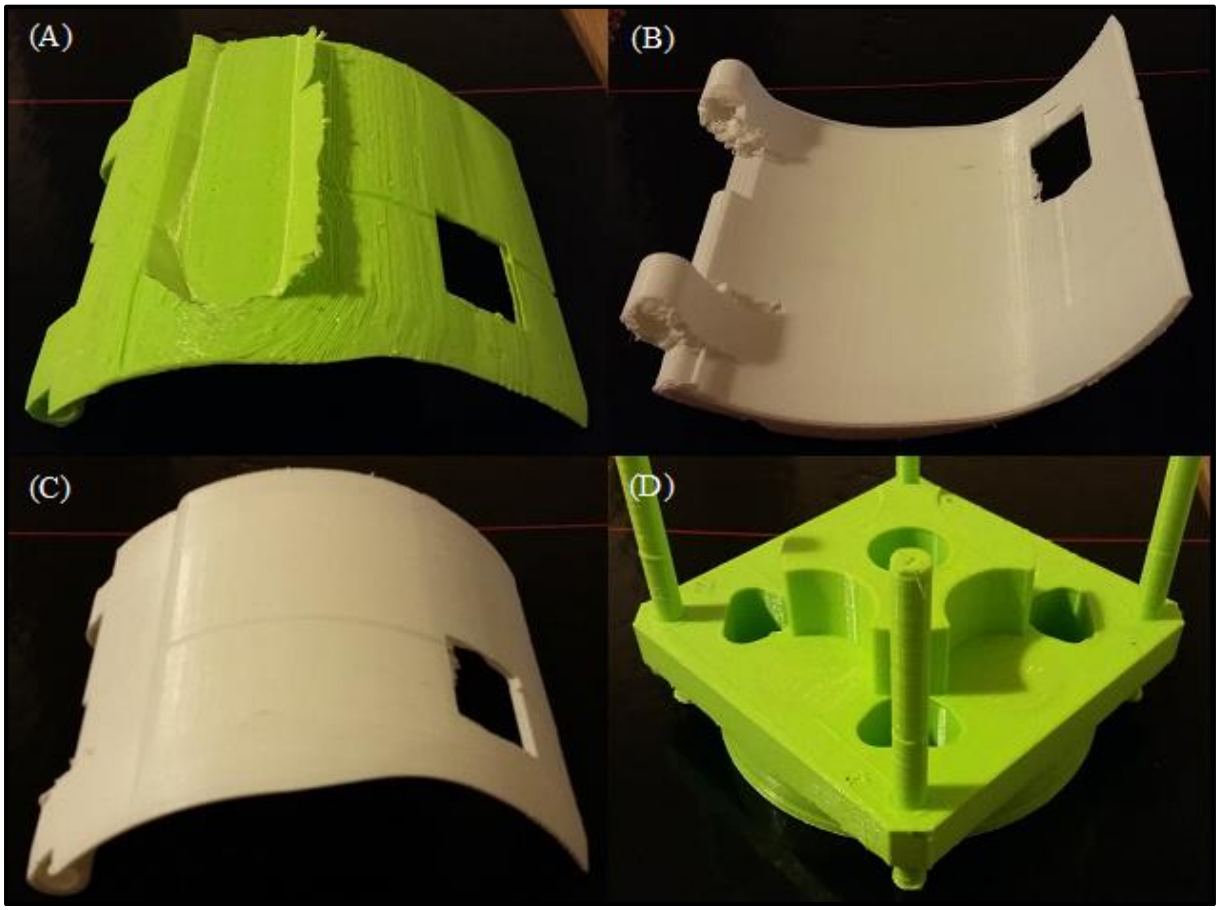

Figure 5.5: Photos of prototypes. (A) Outer face of fin 4. (B) Inner face of fin 8. (C) Outer face of fin 8. (D) Fin cup and hinge pins, printed as one part. These photos do display the key findings from the use of the CubePro®; however, photos of the other prints are available from the author, upon request.

5.4. *Economic Analysis*

Table 5.6: ROM cost quotation from Apsley Precision Engineering Ltd., for the production of aluminium 6063T extended fins using the traditional method, of extrusion and machining. Note that costs are per fin.

Order Quantity	36	50	100	200
Initial Order	£ 380	£ 280	£ 156	£ 104
Repeat Order	-	-	£ 75	£ 60

Table 5.7: ROM cost quotations from AM companies for fin production. Note that costs are per fin.

Material	**Aluminium Filled PA**	**Accura® 55**	**Somos® PerFORM**	**Carbon Filled PA**	**Aluminium ($AlSi_{10}Mg$) Before HT**	**After HT**
Company	Materialise	CRDM	Materialise	Materialise	3TRPD	Materialise
Process	LS	SLA	SLA	LS	LS	3DP
Extended Fin	£ 40	£ 59	£ 187	£ 127	£ 391	£ 330
Current Fin	£ 30	£ 59	£ 170	£ 127	£ 370	£ 330

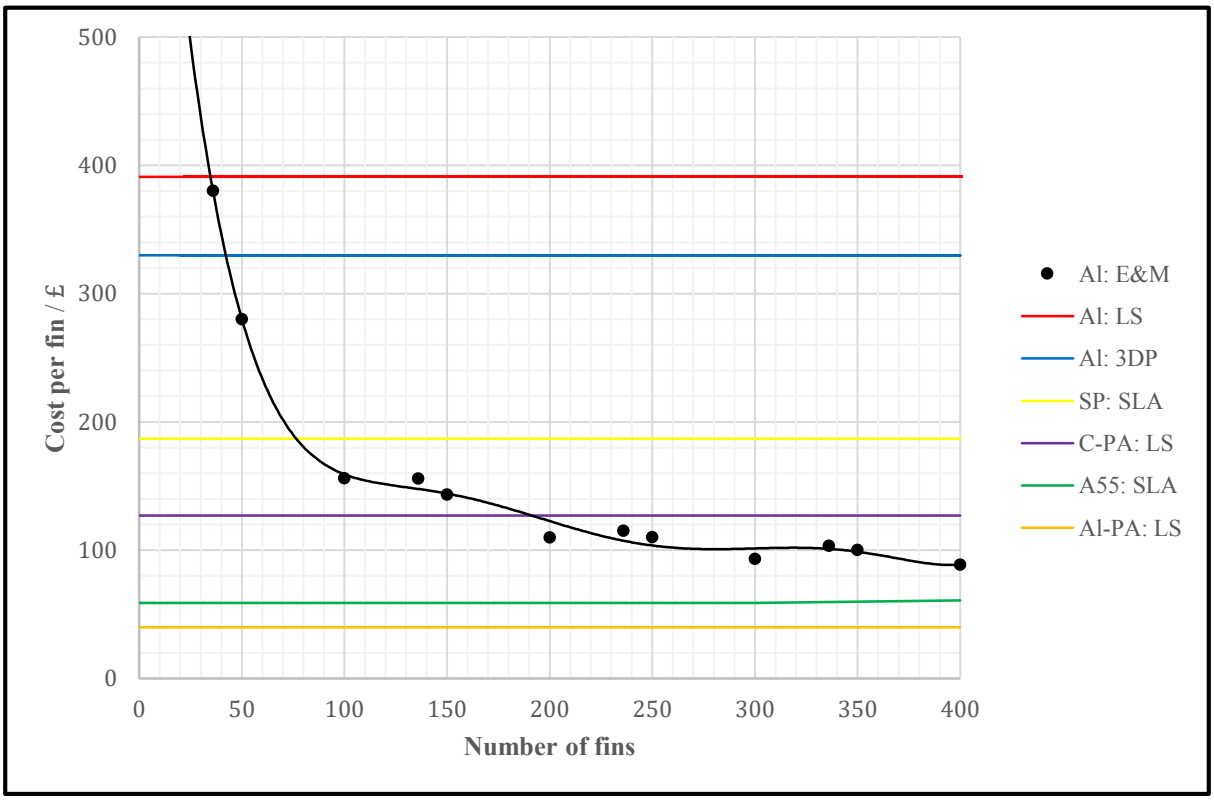

Figure 5.6 Comparison of fin production cost between the traditional production method of extrusion and machining (E&M), and a number of AM processes, namely: laser sintering (LS), stereo-lithography (SLA), and 3D printing (3DP). The materials considered here are: aluminium (Al), Somos® PerFORM (SP), carbon filled nylon (C-PA), aluminium filled nylon (Al-PA), and Accura® 55 (A55).

6. Discussion

6.1. Finite Element Analysis

The major finding from the transient structural FE analysis, is that AM C-PA, available from Materialise, is not suitable for the application of CCM's extended fin. However, based upon the predicted failure location, re-design of the fin may permit the use of C-PA, or even other AM materials with lower strength and stiffness

Candidate AM Materials

The results of the FE analysis show that if the C-PA material is used, it is likely to fail mechanically, during deployment. As table 5.1 displays, the maximum tensile stress was found to be $132\ MPa$; which is greater than the C-PA's UTS of $84\ MPa$, as given in table 3.1. Although, as shown by figure 5.1, there is a high predicted error in the results, regarding the higher tensile stresses; the maximum stress is shown to always be greater than C-PA's UTS by table 5.1.

It is unlikely that a different result would be obtain by undertaking the FE analysis using the material properties for any of the other candidate polymer-based AM materials, given in table 3.1. This is due to the fact that they will all have a similar Poisson's ratio and that the other polymer-based materials have lower tensile strengths than C-PA.

Changes in the result would be expected if the material properties of aluminium were to be used, as the Poisson's ratio would be greater, than that of C-PA. However, assuming the changes in stress to be negligible. The aluminium fins currently employed by CCM operate with a safety factor of 1.85 ± 0.65, which is quite suitable for this application. As aluminium fins are known to consistently withstand the deployment, the obtained safety factor provides validity of the FE analysis; albeit rather crudely. Further validation should be undertaken using actual testing to ensure the results are correct and accurate.

Re-Design of Fin

Due to the high stress regions being located on the sharp edges around the hinge points, as figure 5.2 (B) and (C) show, the maximum values obtained are likely to be a result of stress concentrations. Hence, if the fin was re-designed to remove sharp edges, a much lower stress may be realised. Due to the capabilities of AM, fabricating fins with curved edges to a high accuracy is possible, whereas it may not be through the traditional production method.

6.2. Tensile Testing

Tensile testing of the retaining wire gave an insight into its fracture method, and how this changes with varying strain rates. Moreover, the proposed concept to elimination the retaining wire from the current design, was shown to be feasible through the use of AM.

Fracture Mechanism

Generally, the tensile test results showed the retaining wire to fracture in a more brittle manner as the strain rate was increased. As can be seen in figure 5.4, the lower strain rates, of 50 and $100\ mm \cdot min^{-1}$(trail 1-3, samples 1 and 6), resulted in the fracture taking place over a greater length of wire, with the strands become significantly frayed. Contrastingly, at the higher strain rates, of 750 and $100\ mm \cdot min^{-1}$(samples 4-5, and 9-10), the fracture occurred over a much shorter length of wire, with a clean snap; this can also be observed in figure 5.4. Based upon these observations it is likely that under the launch conditions, the retaining wire fails via the mechanism of fast fracture. Hence, the retaining wire's toughness may have been a more appropriate property to consider than UTS for this analysis.

Elimination of Retaining Wire

In order to eliminate the retaining wire, through an overlapping section joining each fin to next, a suitably small thickness of the candidate AM material is required, as table 5.4 depicts. If this concept was to be implemented through the use of AM; component elimination, reduced labour costs, and improved safety could all be realised.

Component elimination could be achieved as the four fins, and retaining wire, would be replaced by one AM part. This would then reduce the number of parts being assembled, to manufacture the countermeasure; in turn, reducing the direct labour hours required and hence labour costs. Improved safety of launch would also be realised due to the aforementioned unpredictably of the retaining wire's trajectory, once fractured.

Nonetheless, the method used to estimate the UTS of the retaining wire, at the strain rate at launch, provided only a rather crude approximation. As the strain rate of the retaining wire at launch, was itself estimated using equation 3.14, to be orders of magnitude greater than the capabilities of the steady tensile testing. Hence, the results were extrapolated over a large range, and it is unlikely that the same relationship between UTS and strain rate will hold over this range of values. Hence, any design emerging from this research, must be exhaustively tested to ensure functional consistency of fin deployment.

6.3. CubePro® Prototyping

Overall, the CubePro® was successful in fabricating the fin's geometry; with all but one of the nine builds producing a prototype. However, some builds were more successful than others, and the alignment, within the build volume, has been identified as a key parameter.

Alignment of Fin

Six of the eight builds had a vertical alignment, referring to the fin's top edge being located on the platform. The geometry was generally successfully created, as depicted by figures 5.5 (B) and (C). But they also show that the overhanging edges proved difficult to fabricate using the CubePro®. The defects observed were caused by the support structure not being sufficient. Hence, the support structures are a bottleneck of producing fins through the use of an extrusion based system, such as CubePro®. However, it is not envisaged that this would be a problem if PBF or vat photo-polymerisation technologies were used [33]; due to the extra support from the bed of powder or vat of liquid, as oppose to the volume of gas in extrusion based systems.

Fin 4 was built with a horizontal alignment, the outer face was located on the build platform. As figure 5.5 (A) shows this caused an issue with the removal of the support structure, although this did avoid the aforementioned defect regarding the hinges. An attempt to fabricate a fin (fin 6) with only one corner being in contact with the platform was made. However, this failed.

Other Printing Parameters

Fabrication quality was seen to be independent of the material used. However, PLA and ABS, are both thermoplastics with similar properties, so this was to be expected. It is unlikely that a comparison between, say a metal and a polymer, would yield the same conclusion [30].

As expected, lower resolutions led to shorter build times, as seen in table 5.5. As did the use of a honeycomb print pattern, over the diamond structure. In terms of part mass, table 5.5 displays fin 2 having a high mass. This was due to the use of 'lines' for the support, as oppose to 'points'; this resulted in a support structure that was too stiff and strong to be removed.

Component Elimination

The fin cup-hinge pin build underlined further potential for CCM to use AM for component elimination; since the geometry was fabricated with minimal defects, as figure 5.5 (D) shows. The geometry of this build was quite complex; and it would have been much more difficult, let alone wasteful, to produce this part using traditional methods.

6.4. Economic Suitability

The economic analysis, presented in section 5.4, shows that the use of AM to produce aluminium fins is not economically competitive with the traditional method of extrusion and machining. Furthermore, the results of the FE analysis indicated polymer-based material to not be suitable and so AM in general has been shown to not be feasible for fin production.

Aluminium

AM is shown to not be a viable production method for the fins by figure 5.6. Lifetime production quantity would need to be under 46; this would be enough for 11 countermeasures, which would be much less than a single order for CCM. However, if the fins were re-designed to greater utilise the benefits of AM, it may be found to be more cost-effective [18, 19].

Polymer

The production of polymer-based AM fins was shown to be more competitive with the traditional method of extrusion and machining. However, the strongest and stiffest options; Somos® PerFROM and the C-PA, are unlikely to be economically viable, due to their respective breakeven points of 75 and 180 fins, depicted from figure 5.6. The two weaker polymer based options; Accura® 55 and the aluminium filled nylon (A-PA), were shown to provide a cost-benefit for all production volumes, up to at least 400.

Due to the FE analysis, discussed in section 6.1, the C-PA is concluded to not be strong enough. Hence, it is highly unlikely that the weaker Accura® 55 or A-PA materials would be. Nevertheless, if re-designed, polymer-based fins could become mechanically suitable for the fins, as previously discussed. As the economic analysis shows outsourcing the AM of polymers to be lower cost than the traditional method, this could be a viable production solution. On the other hand, the traditional method used was for the production of aluminium fins; and so a traditional method of polymer production is required as a further comparison. However, these techniques, such as injection moulding, tend to suited to mass production; which does not correspond to CCM's volume of manufacture.

Comparison to Literature

As depicted in section 2.3, the literature agrees that the lower the production volume the more economically viable AM is [15-19, 26]. This is also seen in figure 5.6. However, the literature focuses on a company undertaking AM in-house. If CCM were to do this the cost per fin would be much higher initially, but lower once the machine costs are paid off.

7. Conclusions

7.1. Summary of Findings

This project investigated the viability for Chemring Countermeasures to use additive manufacture in the production of their fin components, and the major findings are as follows:

- Carbon filled nylon fins, produced by laser sintering, will mechanically fail at the hinge points during deployment.
- The aluminium fins currently in service operate with a safety factor of 1.85 ± 0.65.
- The retaining wire used to seal the fins before launch fractures in a brittle manner, and this is likely to be via fast fracture.
- The geometry of the fins is suitable for additive manufacture, and the best method is to build from the top edge upwards.
- Outsourcing the additive manufacture of aluminium fins is not economically competitive with the traditional method of extrusion and machining.
- Outsourcing the additive manufacturing of polymer-based fins is economically viable, however, for the current design they will fail mechanically on deployment.

7.2. Recommendations for Future Research

Whilst this project resulted in a number of findings that will hopefully be of direct use to Chemring Countermeasures, it also uncovered many potential topics for further research and discussion. The key recommendations for further study are as follows:

- Re-design of the fin, to create smoother edges. This is likely to reduce the stresses induced in the fins during deployment. Hence allowing polymer-based materials, such as carbon filled nylon, to be suitable for this application; which could yield an economical benefit.
- Validation of finite element results with actual mechanical testing.
- Further mechanical testing of the retaining wire at higher strain rates, potentially considering the toughness as well as the ultimate tensile strength.
- Development of concept to additively manufacture the four fins and retaining wire as a single part, and other designs resulting in component elimination.
- Advancement of cost model to consider assembly and labour costs.
- Development of cost models for fin production by additive manufacturing in-house.

8. Project Management

Throughout this project Ashour Pour et al.'s AM evaluation framework has been used as a basis for the project's structure [3]. Hence, a "*preliminary assessment*" was first undertaken; encompassing the project planning and background reading, which led to the formation of the literature review, and identification of candidate AM materials. Whilst, identifying the need for the subsequent "*technical assessment*" sections of this project, which included the development of the mathematical model, and subsequent FE analysis. But also, the tensile testing and CubePro® 3D printing. Finally the "*economic assessment*" was undertaken.

The progress of this project was managed by a Gantt chart, which is given by table 8.1. As the project developed it became clear that the scope was too ambitious; with the large selection of tasks being too extensive for a project of this size. Hence, the fin design was set as a fixed variable, and materials and process selection parts of the project were focused upon.

In addition, a logbook was employed, to keep a record of all key aspects relevant to the project. Meetings with Dr Gavin Tabor were held on an approximately weekly basis, in order to review progression and obtain advice. Weekly aims and objectives were set, with an estimate for the length of each task. Furthermore, contact with the relevant parties at CCM was maintained throughout the project, through email. In addition, face-to-face meetings were held, at CCM, towards the start and end of the project.

The materials used in this project are highly unlikely the cause any environmental risk. However, the disposal of the polymer prototypes produced from the CubePro® prototyping, at the end of their useful life is important. Both the polymers used, ABS and PLA, are recyclable; therefore when the prototypes are no longer useful they shall recycled. However, if they were bio-degradable, a further sustainability benefit could be realised. This highlights that the development of bio-degradable polymers for rapid prototyping and AM could be very beneficial in the future. It is not envisaged that this project will have an effect on society, and the carbon footprint of this project was negligible.

Prior to this project, it was not envisaged that any risks to the wellbeing of anyone would be created. All of the materials used were non-hazardous. If AM machines or experimental equipment had been used incorrectly, an element of risk would have been presented. In order to avoid this, careful attention was paid to health and safety guidance throughout this project. In doing so, no accidents or incidents occurred, with direct or in-direct relation to this project.

Table 8.1: Project management system in the form of a Gaant chart. Displaying project sections, tasks and milestones. Adapted from [42].

Task Name	Duration	Start	Finish
Materials and process selection	**30 days**	**Mon 11/01/16**	**Fri 19/02/16**
Research AM processes	20 days	Mon 11/01/16	Fri 05/02/16
Research AM materials	20 days	Mon 11/01/16	Fri 05/02/16
Tensile stesting of steel cord	10 days	Mon 11/01/16	Fri 22/01/16
Identify required properties	10 days	Mon 25/01/16	Fri 05/02/16
Materials selection	10 days	Mon 08/02/16	Fri 19/02/16
Material and process selected	0 days	Fri 19/02/16	Fri 19/02/16
Fin design	**30 days**	**Mon 11/01/16**	**Fri 19/02/16**
Concept designs	5 days	Mon 11/01/16	Fri 15/01/16
Computional analysis	10 days	Mon 18/01/16	Fri 29/01/16
Rapid prototyping	5 days	Mon 01/02/16	Fri 05/02/16
Experimental testing	10 days	Mon 08/02/16	Fri 19/02/16
Final design chosen	0 days	Fri 19/02/16	Fri 19/02/16
Manufacture and testing	**25 days**	**Mon 22/02/16**	**Fri 25/03/16**
AM of final design(s)	15 days	Mon 22/02/16	Fri 11/03/16
Testing of final design	10 days	Mon 14/03/16	Fri 25/03/16
Project complete	0 days	Fri 25/03/16	Fri 25/03/16
Final Report	24 days	Mon 28/03/16	Thu 28/04/16
Report hand-in	0 days	Thu 28/04/16	Thu 28/04/16

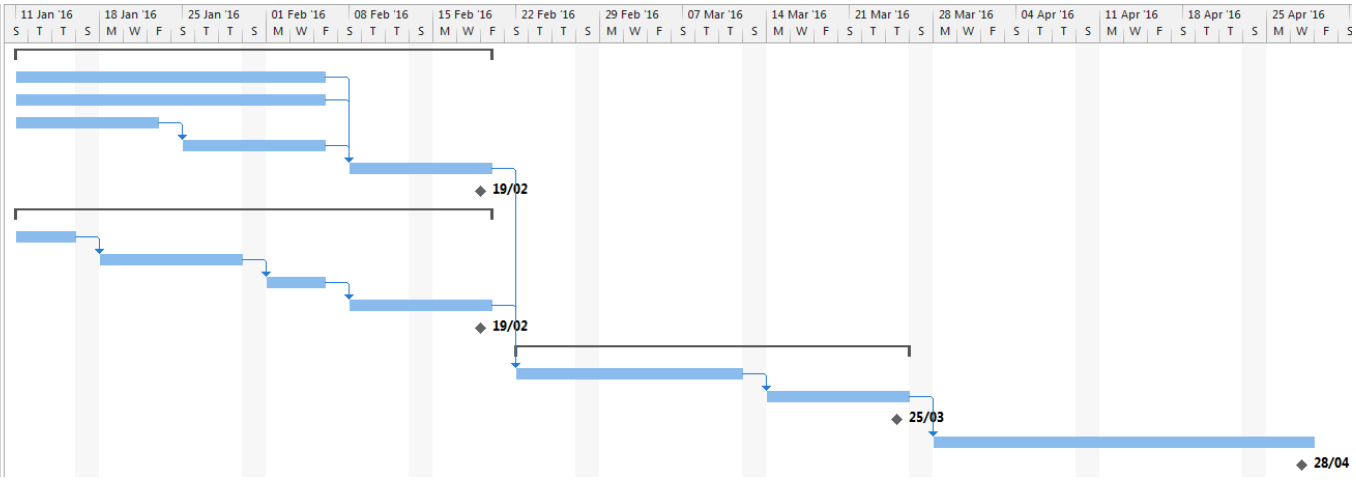

Table 8.2: Risk assessment for the project. Adapted from [42].

Hazard	Effect on People and Project	Consequence (1-5)	Likelihood (1-5)	Risk Score (1-25)	Preventive Action
Design too expensive for manufacture	Unable to manufacture and test design.	5	2	10	Keep track of current and projected costs.
Other modules	Work for other modules delaying progress of this project.	3	3	9	Utilise Gaant chart and keep weekly plan for all work.
Delay in receiving data from CCM	Unable to begin specific project tasks.	4	2	8	Keep CCM updated on progress, and request any data early.
Design uses hazards materials	Manufacture may be unsafe.	5	1	5	Avoid uses hazardous materials unless absolutely necessary.
Lasers used in AM machines	Harmful to operator if direct contact is made with the body.	4	1	4	Follow health and safety procedures when using AM.
Repetitive strain injury	Harmful to the operator, could be long or short term.	3	1	3	Maintain good comfort whilst uses computers for long periods.

References

1. Barlow, A., *Naval Countermeasure Component Study: Final Year Project*. 2015, Chemring Countermeasures Ltd.
2. Gibson, I., D. Rosen, and B. Stucker, *Additive manufacturing technologies: 3D printing, rapid Prototyping, and direct digital manufacturing*. 2014, United States: Springer-Verlag New York.
3. Ashour Pour, M., et al., *An economic insight into additive manufacturing system implementation.* Advances in Production Management Systems: Innovative Production Management Towards Sustainable Growth, 2015: p. 146-155.
4. Minckley, P., *Mk.217 Mod1 Feasibility Study (Phase 2): Wind Tunnel*. 2014, Chemring Countermeasures Ltd.
5. Johnson, B., *On the use of Computational Fluid Dynamics and Kriging for the Trajectory Prediction and Fin Optimisation of a Countermeasure*. 2015, University of Exeter.
6. Frazier, W.E., *Metal additive manufacturing: A review.* Journal of Materials Engineering and Performance, 2014. **23**(6): p. 1917-1928.
7. Kruth, J.P., et al., *Selective laser melting of iron-based powder.* Journal of Materials Processing Technology, 2004. **149**(1-3): p. 616-622.
8. Kruth, J.P., et al., *Consolidation phenomena in laser and powder-bed based layered manufacturing.* CIRP Annals - Manufacturing Technology, 2007. **56**(2): p. 730-759.
9. Murr, L.E., et al., *Metal fabrication by additive manufacturing using laser and electron beam melting technologies.* Journal of Materials Science and Technology, 2012. **28**(1): p. 1-14.
10. Lewis, G.K. and E. Schlienger, *Practical considerations and capabilites for laser assisted direct metal deposition.* Materials and Design, 2000. **21**(4): p. 417-423.
11. Zeng, K., D. Pal, and B. Stucker, *A review of thermal analysis methods in laser sintering and selective laser melting*, in *23rd Annual International Solid Freeform Fabrication Symposium: An Additive Manufacturing Conference*. 2012: Austin, TX: USA. p. 796-814.
12. Dudek, P., *FDM 3D printing technology in manufacturing composite elements.* Archives of Metallurgy and Materials, 2013. **58**(4): p. 1415-1418.
13. Brooks, H. and S. Molony, *Design and evaluation of additively manufactured parts with three dimensional continuous fibre reinforcement.* Materials and Design, 2016: p. 276-283.
14. Meisel, N.A., A.M. Elliott, and C.B. Williams, *A procedure for creating actuated joints via embedding shape memory alloys in PolyJet 3D printing.* Journal of Intelligent Material Systems and Structures, 2014. **26**(12): p. 1498-1512.
15. Hopkinson, N. and P. Dickens, *Rapid prototyping for direct manufacture.* Rapid Prototyping Journal, 2001. **7**(4): p. 197-202.
16. Hopkinson, N. and P. Dickens, *Analysis of rapid manufacturing—using layer manufacturing processes for production.* Proceedings of the Institution of Mechanical Engineers, Part C: Journal of Mechanical Engineering Science, 2003. **217**(1): p. 31-39.
17. Ruffo, M., C. Tuck, and R. Hague, *Cost estimation for rapid manufacturing - laser sintering production for low to medium volumes.* Proceedings of the Institution of Mechanical Engineers, Part B: Journal of Engineering Manufacture, 2006. **220**(9): p. 1417-1427.
18. Atzeni, E., et al., *Redesign and cost estimation of rapid manufactured plastic parts.* Rapid Prototyping Journal, 2010. **16**(5): p. 308-317.
19. Atzeni, E. and A. Salmi, *Economics of additive manufacturing for end-usable metal parts.* The International Journal of Advanced Manufacturing Technology, 2012. **62**(9-12): p. 1147-1155.
20. Baumers, M., et al., *A comparative study of metallic additive manufacturing power consumption*, in *21st Annual International Solid Freeform Fabrication Symposium: An Additive Manufacturing Conference*. 2010: Austin, TX: United States. p. 278-288.
21. Baumers, M., et al., *Combined build-time, energy consumption and cost estimation for direct metal laser sintering*, in *23rd Annual International Solid Freeform Fabrication Symposium: An Additive Manufacturing Conference*. 2012: Austin, TX: United States. p. 932-944.

22. Baumers, M., et al., *Transparancy built-in: Energy consumption and cost estimation for additive manufacturing.* Journal of Industrial Ecology, 2012. **17**(3): p. 418-431.
23. Baumers, M., et al., *The cost of additive manufacturing: Machine productivity, economies of scale and technology-push.* Technological Forecasting and Social Change, 2016. **102**: p. 193-201.
24. Rickenbacher, L., A. Spierings, and K. Wegener, *An integrated cost-model for selective laser melting (SLM).* Rapid Prototyping Journal, 2013. **19**(3): p. 208-214.
25. Manogharan, G., R.A. Wysk, and O.L.A. Harrysson, *Additive manufacturing–integrated hybrid manufacturing and subtractive processes: Economic model and analysis.* International Journal of Computer Integrated Manufacturing, 2015. **29**(5): p. 473-488.
26. Lindemann, C., et al., *Analyzing product lifecycle costs for a better understanding of cost drivers in additive manufacturing*, in *23rd Annual International Solid Freeform Fabrication Symposium: An Additive Manufacturing Conference*. 2012: Austin, TX: United States. p. 177-188.
27. Wohlers, T., *Wohlers Report 2016: 3D printing and additive manufacturing state of the industry annual worldwide progress report*. 2016, Fort Collins, CO: United States: Wohlers Assiocates Inc.
28. Schröder, M., B. Falk, and R. Schmitt, *Evaluation of cost structures of additive manufacturing processes using a new business model.* Procedia CIRP, 2015. **30**: p. 311-316.
29. Thomas, D.S. and S.W. Gilbert, *Costs and cost effectiveness of additive manufacturing: A literature review and discussion*. 2014, National Institute of Standards and Technology: Gaithersburg, MD: United Stated.
30. Deradjat, D. and T. Minshall, *Implementation of additive manufacturing technologies for mass customisation*, in *24th International Association for Management of Technology Conference: Technology, Innovation and Management for Sustainable Growth*. 2015: The WestinCape Town, South Africa. p. 2079-2094.
31. Mellor, S., L. Hao, and D. Zhang, *Additive manufacturing: A framework for implementation.* International Journal of Production Economics, 2014. **149**: p. 194-201.
32. Achillas, C., D. Aidonis, and E. Iakovou, *A methodological framework for the inclusion of modern additive manufacturing into the production portfolio of a focused factory.* Journal of Manufacturing Systems, 2015. **37**: p. 328-339.
33. Nagel, J.K.S. and F.W. Liou, *Manufacturing System*. 2012: InTech.
34. Khajavi, S.H., et al., *Risk reduction in new product launch: A hybrid approach combining direct digital and tool-based manufacturing.* Computers in Industry, 2015. **74**: p. 29-42.
35. 3DSystems. *Accura 55 Plastic*. 2007 03/02/2016]; <http://crdm.co.uk/pdf/Accura_55_plastic_MDS.pdf>].
36. Materialise. *Stereolithography Material Properties*. 2016 08/02/2016]; <http://manufacturing.materialise.com/sites/default/files/public/AMS/Datasheets_January2016/datasheets_stereolithography_2016.pdf>].
37. Materialise. *Metal 3D Printing Material Properties*. 2016 09/02/2016]; <http://manufacturing.materialise.com/sites/default/files/public/AMS/Datasheets_January2016/datasheets_metal3dp_2016.pdf>].
38. Materialise. *Laser Sintering Material Properties*. 2016 15/02/16]; <http://manufacturing.materialise.com/sites/default/files/public/AMS/Datasheets_Jan2016/datasheets_lasersintering_2016.pdf>].
39. 3TRPD. *Material Specification: Aluminium AlSi10Mg*. 2015 29/01/2016]; <http://www.3trpd.co.uk/wp-content/uploads/2015/05/Aluminium-AlSi10Mg.pdf>].
40. Douglas, J.F., et al., *Fluid mechanics*. 6 ed. 2011, Harlow, England: Prentice Hall.
41. Callister, W.D. and D.G. Rethwisch, *Fundamentals of materials science and engineering, SI version*. 4 ed. 2012, United States: John Wiley & Sons.
42. Lewis, P.M., *Suitability for the additive manufacture of countermeasure fin component* 2015, University of Exeter.